Available online www.jsaer.com

***Journal of Scientific and Engineering Research*, 2020, 7(8):114-123**

Research Article

ISSN: 2394-2630
CODEN(USA): JSERBR

Influence of Capacitive Effects on Transformer Windings

Mathurin GOGOM, Désiré LILONGA-BOYENGA

Laboratoire de Génie Electrique et Electronique, Ecole Nationale Supérieure Polytechnique, Université Marien Ngouabi, Brazzaville, Congo

Abstract For years, capacitive effects have been the subject of research. The capacitive effects are the discrete capacitors which appear between the active live line conductors and between them with the ground plane, generating capacitive reactive power. Indeed, it is clear that the geometry of these line conductors influences the determination these capacitors capacities. Similarly, the influence of the reactive energy generated by these capacitors on the transformers located in the upstream and downstream stations of the lines differs depending on whether these transformers windings are coupled in star or in triangle.

This study is carried out to propose an approach which would take into account the geometry of the line conductors and to show how these capacitors influence differently the transformers windings when the coupling of the windings is in star or in triangle. This approach would make it possible to understand in which case the transformers operated in the transport networks can have a long lifespan.

Keywords Capacitive effects, discrete capacitors, geometry of conductors and transformers windings

1. Introduction

The transport of electrical energy between production and consumption centers, often characterized by long distances, poses many problems, among others joule losses and voltage drops. For this purpose, several works have been carried out, in particular the joule losses optimization and voltage drops thanks to traditional and advanced compensation of reactive power [9] and [15]. However, works on the impact of capacitive effects are still very limited, requiring special attention.

Indeed, the reactive energy generated by the discrete capacitors which are created between the different active conductors on the one hand, and between each active conductor with the ground plane on the other hand, varies according to the configuration (geometry) of the line. This reactive energy generated is distributed in half over each of the two ends of the line or cable. When it is not consumed, this reactive energy generated becomes one of the causes of undesirable overvoltage and therefore of instability of the network voltage. These capacitive effects are very harmful during empty or low load operation of the transport network. In addition, these capacitive effects influences differently transformers windings to which are connected the electrical power transport lines. This difference is due to the mode of coupling windings of these transformers.

The formation of these discrete capacitors reflects the capacitive effects on electric lines and cables. The reactive power absorbed by the line inductors or supplied by the capacitors thus formed must obey the requirements of the network, in particular the stability and reliability of the network.

The interest of this work is to show that the capacitive effects influence differently the behavior of the transport network's components, in particular on the transformer because of the geometry of the lines and of the transformers windings's coupling. Therefore, special attention is required when designing these lines and when coupling transformer windings in transport networks.

2. Theoretical study

2.1. Capacitors illustrations

A high voltage power line generates reactive energy because of the capacitors that form between the different conductors on the one hand, and between each conductor and the ground plane on the other hand, as illustrated in Figure1 [3] and [4].

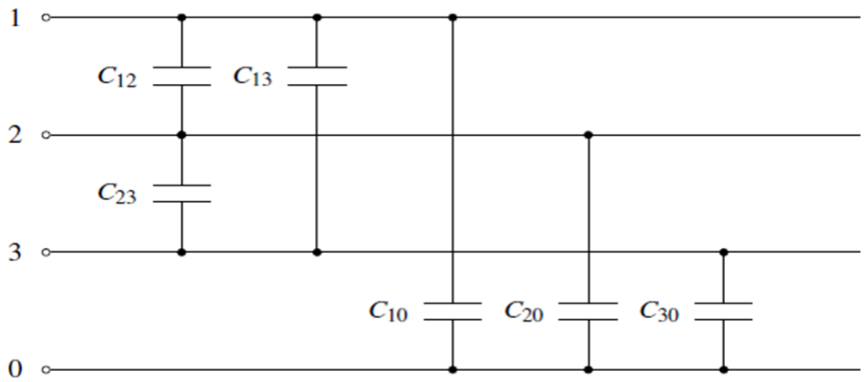

Figure 1: Capacities formed on a power line

Indeed, the capacitor which forms between two conductors (1) and (2) for example, generates reactive power Q_{12} to the network. Between the different line conductors, we have capacitors C_{12}, C_{23} and C_{13}, and between each line conductor and the ground plane the capacitors C_{10}, C_{20} and C_{30}.

2.2. Reactive power generated by capacitors

The example of the plug circuit makes us understand that the capacitor sends its energy on the impedance which is in parallel with it; this allows us to deduce that among the various capacitors formed between the lines conductors, some generate undesirable reactive energy on the transformers windings at the level of the departure and arrival stations when the line is operating at empty or at low load.

The power generated by the capacitor formed between the two conductors (i) and (j) as shown in Figure 2 below, is found in half on each end of the section, that means $Q_{ij}/2$ on each end [3] and [4].

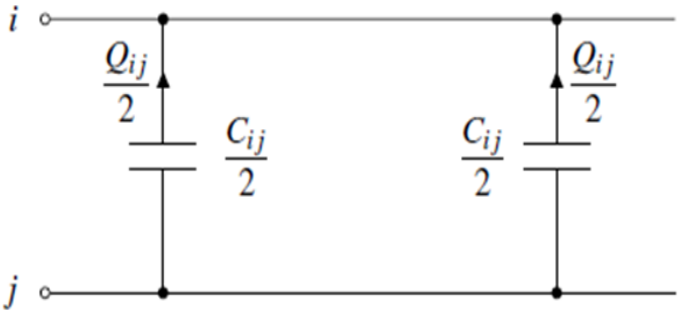

Figure 2: Distribution of reactive energy at the ends of the line

2.2.1. Case of a line supplying the primary of a transformer coupled in triangle

2.2.1.1. Reactive powers generated

It is established that the various capacitors formed between the line conductors appear as reactive energy sources as illustrated in Figure 3. They respectively supply impedances in parallel, in particular the transformer windings.

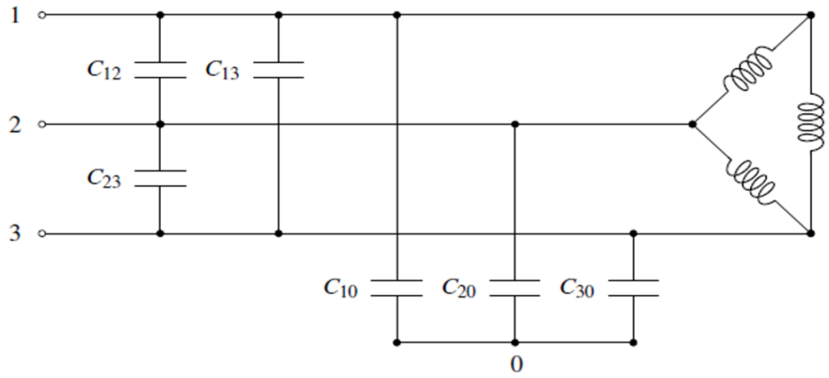

Figure 3: Case of coupling transformer's windings in triangle

For a capacitor created between the active line conductor and the ground plane, the reactive power generated by these different capacitors is located between the phases and the ground plane. This reactive power is that which can be consumed by the equipment which are in parallel with them located at the entrance to the transformer station if these exist. The expression of this reactive power is given by the relation (1) below:

$$Q_{i0} = 3C_{i0}\omega V_{i0}^2 \quad (1)$$

Where V_{i0} is the simple voltage of module $V_{i0} = \frac{U_{12}}{\sqrt{3}} = \frac{U_{13}}{\sqrt{3}} = \frac{U_{23}}{\sqrt{3}}$ and i = 1, 2 and 3;

For the capacitors formed between the guard cables and the ground plane, it can be said that all the energy is earthed, because the two plates constituting this capacitor are earthed; regarding the capacitor created between an active conductor and the guard wire, we find ourselves in the case of a capacitor armature which is connected to earth. Here, we join the previous case where the power generated by the capacitor is sent to earth;

In the case of the capacitor formed between two guard cables, the two armatures of the capacitor thus formed are connected to the ground through pylons. The reactive energy generated is well flowed to the earth;

Regarding the capacitors formed between active conductors, the reactive powers generated by the three capacitors created between the two active conductors of the line are such that:

$$Q_{12} = C_{12}\omega(U_{12})^2, \quad Q_{13} = C_{13}\omega(U_{13})^2 \text{ and } Q_{23} = C_{23}\omega(U_{23})^2 \quad (2)$$

At the start station, this reactive power generated by the capacitors of the line is consumed by the secondary winding of the transformer while at the arrival station, this reactive power is consumed by the primary winding of the transformer at this station. Then we can write:

$$Q_{12} = \frac{U_{12}^2}{L_{12}\omega} \text{ then } L_{12} = \frac{U_{12}^2}{Q_{12}\omega^2} \quad (3)$$

$$Q_{13} = \frac{U_{13}^2}{L_{13}\omega} \text{ then } L_{13} = \frac{U_{13}^2}{Q_{13}\omega^2} \quad (4)$$

$$Q_{23} = \frac{U_{23}^2}{L_{23}\omega} \text{ then } L_{23} = \frac{U_{23}^2}{Q_{23}\omega^2} \quad (5)$$

2.2.1.2. Equivalent capacities of a line

For the purposes of modeling a power line in T or in π, the value of the capacity C to be taken into account per phase is the capacity resulting from the transformation of Figure 4 below.

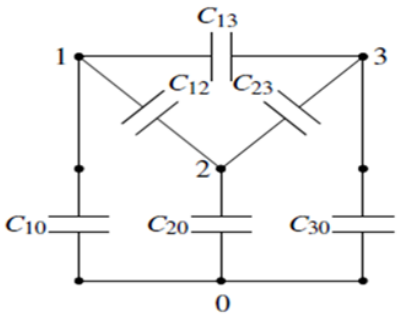

Figure 4: Simplified diagram of a dull simple line

The triangle formed by nodes 1, 2 and 3 can be reduced to the star shape by the triangle-star transformation. The point "n" is at the same potential as the earth, the values of C_{1n}, C_{2n} and C_{3n} are given by:

$$C_{1n} = C_{12} + C_{13} + \frac{C_{12}C_{13}}{C_{23}} \quad (6)$$

$$C_{2n} = C_{12} + C_{23} + \frac{C_{12}C_{23}}{C_{13}} \quad (7)$$

$$C_{3n} = C_{13} + C_{23} + \frac{C_{13}C_{23}}{C_{12}} \quad (8)$$

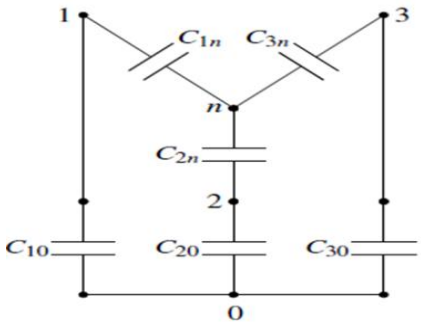

Figure 5: Equivalent diagram in star

We arrive at the final equivalent diagram of figure 6 of which $C_{éq1}$, $C_{éq2}$ and $C_{éq3}$ are given by the expressions below:

$$C_{éq1} = C_{1n} + C_{10} \quad (9)$$

$$C_{éq2} = C_{2n} + C_{20} \quad (10)$$

$$C_{éq3} = C_{3n} + C_{30} \quad (11)$$

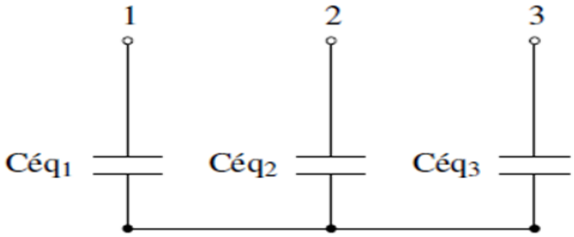

Figure 6: Final equivalent diagram

2.2.2. Case of a line supplying the primary of a star-coupled transformer

2.2.2.1. Reactive power generated

As in the previous case, the different capacitors formed act in the same way. They feed the impedances which are parallel to them.

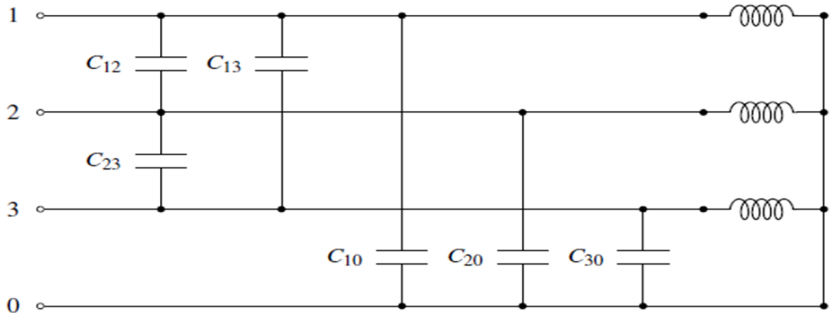

Figure 7: Line supplying the windings of a star-mounted transformer

For a capacitor created between the line active conductor and the ground, the reactive power generated by these different capacitors is located between the phases and the ground. This reactive power is that consumed by half the transformers windings of the upstream and downstream stations of the line. It is given by the relation:

$$Q_{i0} = 3C_{i0}\omega V_{i0}^2 \quad (12)$$

Where V_{i0} is the simple voltage for which the module is given by $V_{i0} = \frac{U_{12}}{\sqrt{3}} = \frac{U_{13}}{\sqrt{3}} = \frac{U_{23}}{\sqrt{3}}$, i = 1, 2 and 3;

As for the capacitors formed between the guard cables and the ground, all of the reactive energy is earthed; Regarding the capacitor created between an active conductor and the guard wire, all reactive energy is discharged to the earth; In the case of the capacitor formed between two guard cables, the reactive energy generated is well drained to the earth; As regards the capacitors formed between two active conductors, the reactive powers generated by each capacitor are such that:

$$Q_{12} = C_{12}\omega(U_{12})^2, \quad Q_{13} = C_{13}\omega(U_{13})^2, \quad Q_{23} = C_{23}\omega(U_{23})^2 \qquad (13)$$

At the start station, half of this reactive power generated by the capacitors formed between line active conductors is consumed by the two secondary windings of the transformer; and at the arrival station, the other half of this reactive power is consumed by the two primary windings of the transformer at this station. Each winding consumes:

$$Q_1 = L_1\omega I_1^2 = \frac{V_1^2}{L_1\omega} \qquad (14)$$

$$Q_2 = L_2\omega I_2^2 = \frac{V_2^2}{L_2\omega} \qquad (15)$$

$$Q_{12} = Q_1 + Q_2 \qquad (16)$$

We deduce successively:

$$Q_{12} = \frac{V_1^2}{L_1\omega} + \frac{V_2^2}{L_2\omega} \qquad (17)$$

$$Q_{13} = \frac{V_1^2}{L_1\omega} + \frac{V_3^2}{L_3\omega} \qquad (18)$$

$$Q_{23} = \frac{V_2^2}{L_2\omega} + \frac{V_3^2}{L_3\omega} \qquad (19)$$

2.2.2.2. Equivalent capacities of a line

For modeling purposes of a power line in T or π, the value of the capacitance C to be taken into account per phase is the capacitance resulting from the transformation of figure 8 below.

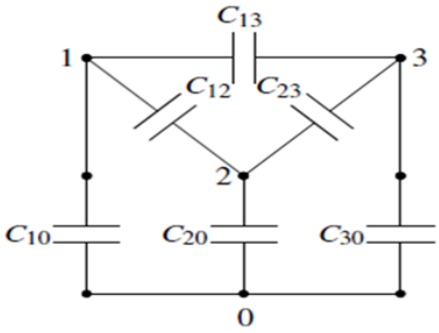

Figure 8: Simplified diagram of a dull single line

The triangle formed by nodes 1, 2 and 3 can be reduced to a star shape by the triangle-star transformation.

The point "n" is at the same potential as the earth, the values of C_{1n}, C_{2n} and C_{3n} are given by:

$$C_{1n} = C_{12} + C_{13} + \frac{C_{12}C_{13}}{C_{23}} \qquad (6')$$

$$C_{2n} = C_{12} + C_{23} + \frac{C_{12}C_{23}}{C_{13}} \qquad (7')$$

$$C_{3n} = C_{13} + C_{23} + \frac{C_{13}C_{23}}{C_{12}} \qquad (8')$$

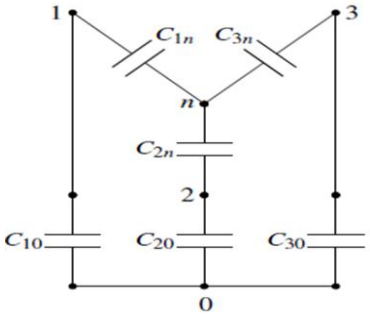

Figure 9: Equivalent diagram in star

We arrive at the following final equivalent diagram:

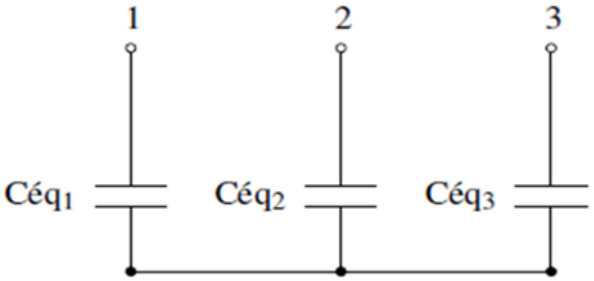

Figure 10: Final equivalent diagram

Under the balanced three-phase regime hypothesis, point n is at the same potential as earth, thus:

$C_{éq1} = C_{1n} + C_{10}$ (9')

$C_{éq2} = C_{2n} + C_{20}$ (10')

$C_{éq3} = C_{3n} + C_{30}$ (11')

2.3. Capacitor capacity expressions

It is a question of giving the expressions of the capacitors capacities formed between the line active conductors on the one hand, and between line active conductor with the ground plane on the other hand by taking into account the geometry of the lines.

The capacity of a capacitor formed between two active conductors is given by [1-2, 7-8]:

$$C_{ij} = \frac{\pi\varepsilon_0}{\log\left[\frac{\frac{D_{ij}}{2}+\sqrt{\frac{D_{ij}^2}{4}+r^2}}{r}\right]} \quad (20)$$

However, that of a capacitor formed between the active conductor and the ground plane is given by[1], [2], [7] et [8]:

$$C_{i0} = \frac{2\pi\varepsilon_0}{\log\left[\frac{h_{i0}+\sqrt{h_{i0}^2+r^2}}{r}\right]} \quad (21)$$

where:

D_{ij}, the distance between two active conductors; r, conductor radius; ε_0, absolute permittivity in a vacuum ($\varepsilon_0 = 8{,}854.10^{-12}\mathrm{F/m}$) and h_{i0}, the distance between the active conductor and the ground plane.

3. Determination of the characteristic quantities of the capacitive effects

3.1. Calculation of reactive capacities and powers

We use formulas (2), (12), (13), (20) and (21) to calculate the capacities and the reactive powers generated C_{ij}, C_{i0}, Q_{ij} and Q_{i0} as a function of the voltage level and the geometry of the single term line conductors; the distance between two active conductors, the radius of the conductor and the distance between the active conductor on the ground plane. The results obtained are reported in Tables 1 and 2 below.

Table 1: Capacitance values of capacitors formed.

	110 KV			**220 KV**		
	Nappe	**Equilateral Triangle**	**Isocel Triangle**	**Nappe**	**Equilateral Triangle**	**Isocel Triangle**
$C_{12}(10^{-12}$ F/m)	10.144	10.144	10.144	9.6136	9.6136	9.6136
$C_{13}(10^{-12}$ F/m)	9.1405	10.144	9.616	8.7076	9.6136	9.1382
$C_{23}(10^{-12}$ F/m)	10.144	10.144	10.144	9.6136	9.6136	9.6136
$C_{10}(10^{-12}$ F/m)	15.198	15.198	14.876	15.251	15.251	14.799
$C_{20}(10^{-12}$ F/m)	15.198	14.647	15.198	15.251	14.501	15.251
$C_{30}(10^{-12}$ F/m)	15.198	15.198	15.198	15.251	15.251	15.251

Table 2: Reactive powers values generated

	110 KV			220 KV		
	Nappe	**Equilateral Triangle**	**Isocel Triangle**	**Nappe**	**Equilateral Triangle**	**Isocel Triangle**
Q_{12}(KVAR/Km)	38.541	38.541	38.541	146.104	146.104	146.104
Q_{13}(KVAR/Km)	34.728	38.541	36.535	132.336	146.104	138.879
Q_{23} (KVAR/Km)	38.541	38.541	38.541	146.104	146.104	146.104
Q_{10}(KVAR/Km)	57.745	57.745	56.522	231.777	231.777	224.923
Q_{20}(KVAR/Km)	57.745	55.651	57.745	231.777	220.376	231.777
Q_{30} (KVAR/Km)	57.745	57.745	57.745	231.777	231.777	231.777

We note, from the results recorded in table 1 above, that the capacities Cij and Ci0 are not the same; they vary according to the geometry of the line conductors. The reactive powers Qij and Qi0 generated vary in the same way. It should also be noted that the reactive power generated by the capacitor formed between the active conductor and the ground plane decreases as the height between them increases. Similarly, that generated by the capacitors formed between active conductors decreases when the distance between them increases.

3.2. Calculation of equivalent capacities and reactive powers

The formulas (6), (7), (8), (9), (10), (11) and (12) enabled us to calculate the equivalent capacities values of the capacitors thus formed for each voltage level. However, formulas (1) and (12) allowed us to calculate the reactive powers generated per phase. The results obtained are presented in Table 3 below.

Table 3: Equivalent capacitance values of the capacitors formed

	110 KV			220 KV		
	Nappe	**Equilateral Triangle**	**Isocel Triangle**	**Nappe**	**Equilateral Triangle**	**Isocel Triangle**
$C_{eq.1}(10^{-12}$ F/m)	43.6235	45.63039	44.2529	42.2799	44.0918	41.8289
$C_{eq.2}(10^{-12}$ F/m)	45.6304	45.07924	46.1872	45.0920	43.3416	44.5919
$C_{eq.3}(10^{-12}$ F/m)	43.6235	45.63039	44.5747	42.2799	44.0918	43.1410

Table 4: Reactive power values generated per phase

	110 KV			220 KV		
	Nappe	**Equilateral Triangle**	**Isocel Triangle**	**Nappe**	**Equilateral Triangle**	**Isocel Triangle**
$Q_{.1}$(KVAR/Km)	165.7431	173.3681	168.1345	672.1592	670.0896	635.6988
$Q_{.2}$(KVAR/Km)	173.3681	171.2741	175.4836	685.2900	658.6884	677.6898
Q_{3}(KVAR/Km)	165.7431	173.3681	169.3571	642.5528	670.0896	655.6396

For each given voltage level, the equivalent capacities C_{eqi} and the reactive powers generated Q_i differ from one geometry of the line conductors to another. Likewise, the equivalent capacities and the reactive powers generated differ from one phase to another. With regard to the results in Table 4, we note that the windings of the transformers consume different reactive powers.

3.3. Example of a radial network

The influence of capacitive effects on the windings of the transformers located upstream and downstream of the lines is examined on the Liouesso-Ouesso network in the Sangha department of the Republic of Congo.

3.3.1. Network Description

The Liouesso-Ouesso electrical network is shown in Figure 11 below. These characteristics are summarized in Table 5.

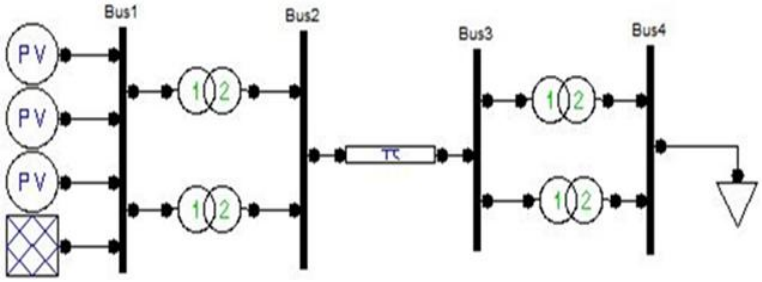

Figure 11: « Liouesso-Ouesso » Electrical network

Table 5: Characteristics of the Liouesso-Ouesso network

Alternateurs				Transformation post of Liouesso				
U_n	$3\times S_n$	$cos\varphi$	$3\times P_n$	U_{1n}	U_{2n}	S_n	U_{ncc}	P_{ncc}
kV	MVA	-	MW	KV	KV	MVA	%	KW
11	23.43	0.85	19.5	11	110	25	10.5	29

Table 5': Continuation of the characteristics of the Liouesso-Ouesso network

Ligne 110 kV				Transformation post of Ouesso				
L	r_0	x_0	b_0	U_{1n}	U_{2n}	S_n	U_{ncc}	P_{ncc}
Km	Ω/Km	Ω/Km	Ω^{-1}/Km	KV	KV	MVA	%	KW
120	0.17	0.39	$2.95.10^{-6}$	110	20	25	10.5	60

3.3.2. Network modeling

We possibly choose the basic voltage and power to transcribe the network parameters in pu [9]. So, U_B = 110 KV; S_B = 100 MVA and we deduce the basic impedance and admittance such as: $Z_B = \frac{U_B^2}{S_B}$ and $Y_B = \frac{S_B}{U^2{}_B}$.

These parameters are presented in Table 6 and 7 below:

Table 6: Longitudinal and transverse parameters of the line in pu

n^0	Sections	R	X	G	B
1	1-2	0.025	0.27	0	0
2	2-3	0.17	0.4	0	0.43
3	3-4	0.012	0.09	0	0

Table 7: Active and reactive powers at the nodes of the pu network

n^0	P_G	Q_G	P_C	Q_C
1	0	0		
2			0	0
3			0	0
4			0	0

3.3.3. Simulations, Results and Discussion

The simulations are performed during no-load operation using the Newton-Raphson algorithm implemented in Matlab [9]. The results obtained are presented in the following table. The related voltage histogram is also shown in Figure 12.

Table 8: Voltage modules and phases, then powers generated and consumed at the nodes in pu

n^0	V	φ	P_G	Q_G	P_C	Q_C
1	1.0200	0	0.0195	-0.5323		
2	1.1606	-0.0157			0	0
3	1.2688	-0.0556			0	0
4	1.2688	-0.0556			0	0

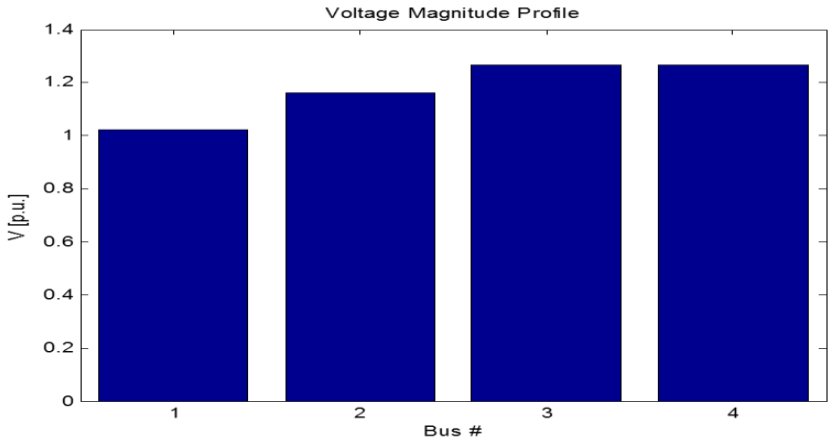

Figure 12: Voltage profile at different nodes

From the results obtained, we can deduce the reactive powers generated by the capacitors formed between conductors using formula (2). These are presented in Table 9 below. At the end of these deductions, we will appreciate the influence of these capacitive effects on the transformers windings located upstream and downstream of the line.

Table 9: Reactive powers generated during no-load operation

	110 KV		
	Nappe	**Equilateral Triangle**	**Isocel Triangle**
Q_{12}(MVAR)	7.4454	7.4454	7.4454
Q_{13}(MVAR)	6.7089	7.4454	7.0579
Q_{23}(MVAR)	7.4454	7.4454	7.4454

3.3.4. Inductance deduction

It is interesting to appreciate the inductances of the transformers windings which consume the reactive energy generated by the capacitors thus formed. The consumption of this energy varies according to the coupling of the windings.

3.3.4.1. Case of triangle coupling of windings

By applying formulas (3), (4) and (5), we obtain the results given in table 10 below:

Table 10: Inductances values of the windings transformer

	110 KV		
	Nappe	**Equilateral Triangle**	**Isocel Triangle**
L_{12}(H)	8.3321	8.3321	8.3321
L_{23}(H)	8.3321	8.3321	8.3321
L_{13}(H)	9.2468	8.3321	8.7895

3.3.4.2. Star coupling Case of windings

Assuming that the system is symmetrical, solving equations (17), (18) and (19) allows us to obtain the results recorded in table 11 below:

Table 11: Inductances values of the transformer's windings

	110 KV		
	Nappe	**Equilateral Triangle**	**Isocel Triangle**
L_1(H)	2.777	2.777	2.777
L_2(H)	3.082	2.777	2.929
L_3(H)	2.777	2.777	2.777

The examination of the results recorded in Tables 10 and 11 show that the geometry of the conductors in an equilateral triangle guarantees the symmetry of the three-phase system; however, the star coupling is more expensive, because the windings of this one can have a number of turns $\sqrt{3}$ times less than that of the transformer whose coupling of the windings is in triangle.

4. Conclusion

In our study, we first of all modeled the line, essentially representing the capacitive effects between active conductors on the one hand, and between active conductors and the ground on the other. Then, we calculated the capacities of the discrete capacitors. Likewise, equivalent capacities have been deducted. Finally, the examination of the influence of these capacitive effects on the transformer windings has been done on the radial electrical network existing in the Republic of Congo. The results obtained show that:

- the discrete capacitors capacities and the reactive energies generated by these capacitors are different;
- the capacitive effects influence the transformer windings differently depending on whether the coupling is in a triangle or a star
  - for triangle coupling, the winding of the transformer winding consumes all of the energy generated;
  - For star coupling, the energy generated is consumed by the two windings of the transformer windings.

In short, the design of line conductors in an equilateral triangle is better than the other models when we want to guarantee the symmetry of the three-phase system. However, the star coupling has more advantage compared to

the triangle coupling, the number of turns of the windings can be reduced by √3 times and the inductance of the winding will be 3 times smaller; and therefore the mass of the transformer will be optimal.

References

[1]. Haddad LYAZID et Hami KHODIR. Calcul des paramètres et caractéristiques des lignes électriques triphasées. Mémoire de Master 2 génie électrique,Université Abderrahmane mira – BEJAÏA, année 2014/2015.

[2]. Théodore WILDI et Gilbert SIBILLE. Electrotechnique 4e édition

[3]. Haroun Abba Labane, Alphonse Omboua, Capacitive dividers on the high voltage lines, International Journal of Engineering and Advanced Research Technology (IJEART) ISSN: 2454-9290, Volume 2, Issue 10, October 2016, pp. 26-32.

[4]. Haroun Abba Labane, Alphonse Omboua, Désiré Lilonga-Boyenga, Capacitive Effects on Electrical Lines and Cables, International Journal of Engineering Science Invention (IJESI) ISSN: 2319–6726, Volume 6, Issue 10, October 2017, pp. 25-32.

[5]. Abdelkader SAYAH. Analyse des Terminaisons d'Eau. Thèse de l'Université des Sciences et de la Technologie d'Oran Mohamed Boudiaf. Année 2016-2017.

[6]. Alphonse Omboua. Soutirage de l'énergie le long des lignes à haute tension : technologie profitable pour les pays en développement,International Journal of Innovation and Applied Studies, ISSN 2028-9324 Vol. 20 No. 1 Apr. 2017, pp. 349-357.

[7]. Patrick LAGONOTTE. Les lignes et des câbles électriques. Chapitre 10 du cours de réseaux électrique.

[8]. Nabila YALAOUI. Calcul de la matrice d'impédances linéiques du système ligne-câble avec la méthode des éléments finis. Mémoire du diplôme de Maitrise ès sciences appliquées soutenu en 2017.

[9]. Mathurin GOGOM, Mavie MIMIESSE, Germain NGUIMBI, Désiré LILONGA-BOYENGA. Improving Availability of Transit Capacity by the Hybrid Optimization Method. Journal of Scientific and Engineering Research, 2018, 5(9): 1-13.

[10]. Flavius Dan Surianu, 2009, Determination of the Induced Voltages bby 220 kV electric overhead power lines working in parallel and narrow routes. Measurements on the ground and mathematical model, WSEAS Transactions on Power Systems, Issue 8, Volume 4, pp.264-274.

[11]. Chebbi Souad, Réseaux électriques en ses divers régimes Cours, Université Virtuelle de Tunis, pp.23,27.

[12]. Boukhenoufa F., Boukadoum A., Leulmi A., et al., Régulation optimale de la tension & compensation de la puissance réactive avec contraintes de sécurité, d'un réseau électrique, par la méthode hybride MPI & AG, Université du 20 Août 1955 et Université Ferhat A., Skikda-Sétif (Algérie) pp.1-6.

[13]. Amidou Betie. Impacts de la qualité du système d'isolation sur la condition et l'efficacité des transformateurs de puissance, Thèse de l'Université du Québec 2015.

[14]. D. Fulchiron. Surtensions et coordination de l'isolement. Cahier Technique Merlin Gerin n° 151. Édition décembre 1992.

[15]. Guillaume Rami. Contrôle de tension auto adaptatif pour des productions décentralisées d'énergies connectées au réseau électrique de distribution, thèse de l'INPG 2006.

[16]. Jean-Marie Escane, Pierre Escane. Modélisation des lignes et câbles, Techniques de l'ingénieur 2001.